Available online at www.sciencedirect.com
ScienceDirect
Journal of Sound and Vibration 322 (2009) 184–195
JOURNAL OF SOUND AND VIBRATION
www.elsevier.com/locate/jsvi

Fluid–structure interaction analysis by optimised boundary element—finite element coupling procedures

Delfim Soares Jr.

Structural Engineering Department, Federal University Of Juiz De Fora, Cidade Universitária, Cep 36036-330, Juiz De Fora, MG, Brazil

Received 4 December 2007; received in revised form 20 October 2008; accepted 7 November 2008
Handling Editor: S. Bolton
Available online 1 January 2009

Abstract

In the present work, fluid–structure interaction problems are analysed by means of optimised boundary element–finite element coupling procedures. The boundary element method is here employed to numerically model acoustic fluids and the finite element method is applied to discretise dynamic bodies (nonlinear effects included). Boundary element—finite element coupling is accomplished by an iterative algorithm: each boundary element or finite element sub-domain is analysed independently (as an uncoupled model) and a successive renewal of the variables at the common interfaces is performed, until convergence is achieved. The evaluation of an optimised relaxation parameter is introduced taking into account the minimisation of a square error functional. The algorithm that arises is more efficient and stable, representing an advancement of the iterative procedure. At the end of the paper, numerical examples are presented, illustrating the potentialities of the proposed methodology.

1. Introduction

Numerical analysis of fluid–structure coupled systems is a complex task, requiring proper treatment of sub-domains in which different physical phenomena are involved, as well as suitable numerical modelling of wave propagation across arbitrary shaped interfaces.

In the present work, two distinct methods are considered in order to numerically discretise the different sub-domains of the fluid–structure coupled model, namely: the boundary element and finite element method. As it is well known, the finite element method is well suited for modelling inhomogeneous and anisotropic solids, as well as for dealing with nonlinear behaviour. The boundary element method, on the other hand, is an appropriate numerical tool to discretise acoustic fluids with infinite extension and/or high gradient concentrations. Thus, coupling boundary and finite element procedures allows the combination of several advantages, which is beneficial for fluid–structure interaction analysis.

Considering time-domain fluid–structure interaction modelling, most of the boundary element and finite element coupling algorithms [1–7] are formulated in a way that a coupled system of equations is established, which afterwards has to be solved using a standard direct solution scheme. Such a procedure leads to several

E-mail address: delfim.soares@ufjf.edu.br

0022-460X/$ - see front matter © 2008 Elsevier Ltd. All rights reserved.
doi:10.1016/j.jsv.2008.11.026

problems with respect to accuracy and efficiency. First, the coupled system of equations has a banded symmetric structure only in the finite element method part, while in the boundary element method part it is non-symmetric and fully populated. Consequently, for its solution the optimised solvers usually used by the finite element method cannot be employed anymore, which leads to rather expensive calculations with respect to computer time. Second, the duration of a time-step needs to be the same in all sub-domains. In general, however, the velocities of the propagating waves in the solid and the fluid are quite different, such that a unified time step may cause serious problems in the numerical solution algorithms (instabilities, lack of accuracy etc.). Third, in the case of taking into account some nonlinearity within the finite element sub-domains, the rather big coupled system of equations needs to be solved in each step of the iterative process, i.e., a few times within each time step. This is very computer time consuming.

Recently, an iterative boundary element—finite element coupling algorithm was developed by Soares et al. [8–10] in order to treat fluid–structure coupled models. Iterative coupling approaches allow boundary element and finite element sub-domains to be analysed separately, leading to smaller and better-conditioned systems of equations (different solvers, suitable for each sub-domain, may be employed). Moreover, a small number of iterations are required for the algorithm to converge and they can be carried out together with the nonlinear analysis (boundary element equations do not need to be dealt with in each step of the nonlinear process). Considering time dependent problems, the stability of the numerical algorithm is also greatly improved, as it is straightforward to use different time-steps (as well as independent spatial discretisations) for sub-domains with different properties. Thus, as has been previously reported [8–10], iterative boundary element—finite element coupling is an efficient and appropriate numerical methodology to deal with time-domain fluid–structure interaction problems.

In the present work an optimised iterative boundary element—finite element coupling algorithm is presented. A square error functional is minimised and an expression for an optimal relaxation parameter is deduced. In fact, the effectiveness of the iterative coupling algorithm is closely related to the relaxation parameter selection: an inappropriate selection can drastically increase the number of iterations in the analysis or, even worse, make convergence unfeasible. As it has been previously reported for some non-transient analysis [11,12], an optimal relaxation parameter selection is extremely case dependent: it depends on the geometry and physical properties of the model, discretisation adopted, boundary conditions etc. The present work proposes a simple expression to optimise the convergence of the iterative process, leading to a more efficient and robust boundary element—finite element coupling technique.

At the end of the paper, numerical examples are considered, illustrating the decrease in the number of iterations when optimised relaxation parameters are adopted, as well as the complex dynamic behaviour of these parameters along typical fluid–structure interaction analysis by means of boundary element—finite element coupled procedures.

2. Boundary and finite element procedures

In the present section, the boundary and finite element basic equations are presented. The boundary element method is here applied to numerically discretise acoustic fluids and the finite element method is employed to model dynamic bodies (nonlinear effects included). Only a very short description concerning the fluid and solid sub-domain modelling is presented next; more details can be found in Refs. [13–18]. In the text that follows, right and left superscripts stand for time and iterative indexes, respectively, and right subscripts stand for a sub-domain reference (as for instance, subscript B or F indicates that a variable is related to a sub-domain modelled by the boundary element or finite element method, respectively).

2.1. Fluid modelling

Taking into account boundary element discretisations, acoustic fluids may be analysed by the following system of equations:

$$\mathbf{C}\mathbf{P}^{t_n} = \sum_{m=1}^{n} (\mathbf{G}^{t_{n-m+1}}\mathbf{Q}^{t_m} - \mathbf{H}^{t_{n-m+1}}\mathbf{P}^{t_m}) + \mathbf{D}^{t_n}, \tag{1}$$

where $\mathbf{P}^{t_n}$ and $\mathbf{Q}^{t_n}$ stand for hydrodynamic pressure and flux vectors, respectively, at time t_n; $\mathbf{C}$ is a point location matrix and $\mathbf{G}^{t_n}$ and $\mathbf{H}^{t_n}$ are influence matrices. Vector $\mathbf{D}^{t_n}$ accounts for domain terms, as for instance initial conditions and/or body source contributions.

By re-arranging the system of Eqs. (1), taking into account the boundary conditions of the problem, the following system of equations arises:

$$\mathbf{A}_B\mathbf{X}^{t_n} = \mathbf{B}_B\mathbf{Y}^{t_n} + \mathbf{Z}^{t_n}, \tag{2}$$

where $\mathbf{X}^{t_n}$ is a vector standing for unknown pressures and fluxes and vector $\mathbf{Y}^{t_n}$ stands for the according known nodal values; $\mathbf{A}_B$ and $\mathbf{B}_B$ are boundary element effective matrices and vector $\mathbf{Z}^{t_n}$ accounts for boundary (and domain, if it is the case) time-convolution contributions. Eqs. (1)–(2) enable the computation of the time-domain boundary element method response at time t_n; they are the basis for the boundary element—finite element coupling scheme concerning the fluid sub-domain.

2.2. Solid modelling

Taking into account a finite element discretisation, the governing system of equations describing a nonlinear dynamic model is given by

$$\mathbf{M}^{(k+1)}\ddot{\mathbf{U}}^{t_n} + \mathbf{C}^{(k+1)}\dot{\mathbf{U}}^{t_n} + \mathbf{K}_T^{(k+1)}\Delta\mathbf{U} = \mathbf{F}^{t_n} - {}^{(k)}\mathbf{R}^{t_n}, \tag{3a}$$

$${}^{(k+1)}\mathbf{U}^{t_n} = {}^{(k)}\mathbf{U}^{t_n} + {}^{(k+1)}\Delta\mathbf{U}, \tag{3b}$$

where $\mathbf{M}$, $\mathbf{C}$, and $\mathbf{K}_T$ are mass, damping and nonlinear stiffness matrices, respectively. The nonlinear residual vector is represented by $\mathbf{F}^{t_n} - {}^{(k)}\mathbf{R}^{t_n}$ and ${}^{(k+1)}\Delta\mathbf{U}$ is the variation of the incremental displacements, calculated at each iterative step. ${}^{(k+1)}\mathbf{U}^{t_n}$, ${}^{(k+1)}\dot{\mathbf{U}}^{t_n}$ and ${}^{(k+1)}\ddot{\mathbf{U}}^{t_n}$ are the displacement, velocity and acceleration vectors, respectively, at time t_n and iterative step $(k+1)$. After considering a time integration scheme (e.g., the Newmark method), an effective system of equations can be obtained, as described by

$$\mathbf{A}_F^{(k+1)}\Delta\mathbf{U} = {}^{(k)}\mathbf{B}_F, \tag{4}$$

which must be solved at each iterative step. In Eq. (4), $\mathbf{A}_F$ is the finite element method effective nonlinear stiffness matrix and ${}^{(k)}\mathbf{B}_F$ is the effective residual vector. Eqs. (3)–(4) enable the computation of the transient finite element method response at time t_n; they are the basis for the boundary element—finite element coupling scheme concerning the solid sub-domain.

3. Coupling of boundary elements and finite elements

In the present work, each boundary element or finite element sub-domain is analysed independently (as an uncoupled model) and a successive renewal of the variables at the common interfaces is performed, through an iterative procedure, until convergence is achieved.

For a fluid–structure interaction problem, the boundary conditions at coupling interfaces, taking into account boundary and finite element formulations, are given by

$$T(\mathbf{F}_F^{t_n})_i = \mathbf{0}, \tag{5a}$$

$$N(\mathbf{F}_F^{t_n})_i + (\bar{\mathbf{P}}_B^{t_n})_i = \mathbf{0}, \tag{5b}$$

$$N(\ddot{\mathbf{U}}_F^{t_n})_i - (1/\rho)(\mathbf{Q}_B^{t_n})_i = \mathbf{0}, \tag{5c}$$

where functions $T(\cdot)_i$ and $N(\cdot)_i$ lead to the tangential and to the normal component of their arguments, respectively, at a node i of the common boundary—finite element interface. In Eq. (5b)—in order to obtain consistency between finite element and boundary element formulations—$\bar{\mathbf{P}}$ represents the equivalent nodal hydrodynamic pressure force, which is obtained from the pressure distribution $\mathbf{P}$. In Eq. (5c), ρ stands for the mass density of the fluid.

In the iterative coupling approach being considered, natural boundary conditions are prescribed, at the common interfaces, for each sub-domain (either modelled by the boundary or finite element method). The accelerations evaluated at the sub-domains modelled by the finite element method are used to obtain the fluxes (prescribed interface boundary condition) for the sub-domains modelled by the boundary element method (Eq. (5c)) and the pressures evaluated at the sub-domains modelled by the boundary element method are used to obtain the nodal forces (prescribed interface boundary condition) for the sub-domains modelled by the finite element method (Eqs. (5a) and (5b)). Concisely, each sub-domain is analysed separately ($\ddot{\mathbf{U}}_F^{t_n}$ and $\mathbf{P}_B^{t_n}$ are evaluated at each iterative step) and the interface relations $\ddot{\mathbf{U}}_F^{t_n} \rightarrow \mathbf{Q}_B^{t_n}$ and $\mathbf{P}_B^{t_n} \rightarrow \mathbf{F}_F^{t_n}$ are iteratively considered until convergence is achieved. A basic algorithm solution for the boundary element—finite element iterative coupling is described in Table 1.

In order to consider different time-steps in each sub-domain, interpolation/extrapolation procedures along time may be considered, as it is described in the fourth and sixth steps of the algorithm presented in Table 1 (β_j and ζ_j stand for time interpolation/extrapolation coefficients). Space interpolation procedures may also be adopted in order to consider independent boundary/finite element method meshes (i.e., disconnected boundary element and finite element interface nodes); this can be accomplished by considering proper interface functions $N_B(\cdot)$ and $\bar{N}_F^{-1}(\cdot)$. In the third step of the algorithm, $N_B(\cdot)$ evaluates normal components at boundary element interface nodes considering interpolation of its argument spatial distribution. In the seventh step, analogous procedures are considered by $\bar{N}_F^{-1}(\cdot)$, which additionally compute nodal equivalent values. Using space/time interpolation/extrapolation procedures, optimal modelling of each sub-domain may be achieved, which is very important in what concerns flexibility, efficiency, accuracy and stability aspects.

As it is described in the second step of the algorithm, a relaxation parameter α is considered in order to ensure and/or to speed up convergence. The effectiveness of the coupling algorithm is intimately related to this relaxation parameter selection: an inappropriate choice for α can drastically increase the number of iterations in the analysis or, even worse, make convergence unfeasible. An optimal relaxation parameter selection, however, is extremely case dependent: it is function of the physical properties of the model, geometric aspects, adopted spatial and temporal discretisations etc. [8,11,12]. In the next sub-section, a simple expression for an optimal relaxation parameter is proposed, considering fluid–structure coupled analyses.

3.1. Optimal relaxation parameter

In order to evaluate an optimal relaxation parameter, the following square error functional is here minimised:

$$f(\alpha) = ||^{(k+1)}\mathbf{Q}_B^{t_B}(\alpha) - {}^{(k)}\mathbf{Q}_B^{t_B}(\alpha)||^2. \tag{6}$$

Taking into account the relaxation of the fluxes for the $(k+1)$ and (k) iterations, Eqs. (7a) and (7b) may be written, regarding steps 2–4 of the coupling algorithm:

$${}^{(k+1)}\mathbf{Q}_B^{t_B} = \beta_0 \rho \mathbf{N}_B({}^{(k+1)}\ddot{\mathbf{U}}_F^{t_F}) + \mathbf{Q}' = \beta_0 \rho \mathbf{N}_B(\alpha^{(k+\alpha)}\ddot{\mathbf{U}}_F^{t_F} + (1-\alpha)^{(k)}\ddot{\mathbf{U}}_F^{t_F}) + \mathbf{Q}', \tag{7a}$$

Table 1
Steps for the iterative boundary element—finite element coupling algorithm.

(1) Finite element sub-domains analyses: evaluation of ${}^{(k+\alpha)}\ddot{\mathbf{U}}_F^{t_F}$ at common interfaces
(2) Adoption of a relaxation parameter: ${}^{(k+1)}\ddot{\mathbf{U}}_F^{t_F} = \alpha^{(k+\alpha)}\ddot{\mathbf{U}}_F^{t_F} + (1-\alpha)^{(k)}\ddot{\mathbf{U}}_F^{t_F}$
(3) Flux–acceleration compatibility (spatial interpolation): ${}^{(k+1)}\mathbf{Q}_B^{t_F} = \rho \mathbf{N}_B({}^{(k+1)}\ddot{\mathbf{U}}_F^{t_F})$
(4) Flux temporal interpolation/extrapolation: ${}^{(k+1)}\mathbf{Q}_B^{t_B} = \beta_0 {}^{(k+1)}\mathbf{Q}_B^{t_F} + \sum_{j=1}^{J_B} \beta_j \mathbf{Q}_B^{(t-j\Delta t)_{B/F}}$
(5) Boundary element sub-domains analyses: evaluation of ${}^{(k+1)}\mathbf{P}_B^{t_B}$ at common interfaces
(6) Pressure temporal extrapolation/interpolation: ${}^{(k+1)}\mathbf{P}_B^{t_F} = \zeta_0 {}^{(k+1)}\mathbf{P}_B^{t_B} + \sum_{j=1}^{J_F} \zeta_j \mathbf{P}_B^{(t-j\Delta t)_{F/B}}$
(7) Force–pressure compatibility (spatial interpolation): ${}^{(k+1)}\mathbf{F}_F^{t_F} = -\bar{\mathbf{N}}_F^{-1}({}^{(k+1)}\mathbf{P}_B^{t_F})$
(8) Check for convergence (go back to step 1 if convergence is not achieved)

$$^{(k)}\mathbf{Q}_B^{t_B} = \beta_0\rho N_B(^{(k)}\ddot{\mathbf{U}}_F^{t_F}) + \mathbf{Q}' = \beta_0\rho N_B(\alpha^{(k+\alpha-1)}\ddot{\mathbf{U}}_F^{t_F} + (1-\alpha)^{(k-1)}\ddot{\mathbf{U}}_F^{t_F}) + \mathbf{Q}', \tag{7b}$$

where $\mathbf{Q}'$ stands for previous time-step flux contributions according to the time interpolation/extrapolation procedure in focus.

Substituting Eqs. (7) into Eq. (6) yields:

$$\begin{aligned} f(\alpha) &= (\beta_0\rho)^2||\alpha^{(k+\alpha)}\mathbf{W}_F^{t_F} + (1-\alpha)^{(k)}\mathbf{W}_F^{t_F}||^2 \\ &= (\beta_0\rho)^2(\alpha^2||^{(k+\alpha)}\mathbf{W}_F^{t_F}||^2 + 2\alpha(1-\alpha)(^{(k+\alpha)}\mathbf{W}_F^{t_F}, ^{(k)}\mathbf{W}_F^{t_F}) \\ &\quad + (1-\alpha)^2||^{(k)}\mathbf{W}_F^{t_F}||^2), \end{aligned} \tag{8}$$

where the inner product definition is employed (e.g., $(\mathbf{W},\mathbf{W}) = ||\mathbf{W}||^2$) and new variables, as defined in Eq. (9), are considered:

$$^{(k+\lambda)}\mathbf{W}_F^{t_F} = N_B(^{(k+\lambda)}\ddot{\mathbf{U}}_F^{t_F}) - N_B(^{(k+\lambda-1)}\ddot{\mathbf{U}}_F^{t_F}). \tag{9}$$

To find the optimal α that minimises the functional $f(\alpha)$, Eq. (8) is differentiated with respect to α and the result is set to zero, as described below:

$$\alpha||^{(k+\alpha)}\mathbf{W}_F^{t_F}||^2 + (1-2\alpha)(^{(k+\alpha)}\mathbf{W}_F^{t_F}, ^{(k)}\mathbf{W}_F^{t_F}) + (\alpha-1)||^{(k)}\mathbf{W}_F^{t_F}||^2 = 0. \tag{10}$$

Re-arranging the terms in Eq. (10), yields:

$$\alpha = (^{(k)}\mathbf{W}_F^{t_F}, ^{(k)}\mathbf{W}_F^{t_F} - ^{(k+\alpha)}\mathbf{W}_F^{t_F})/||^{(k)}\mathbf{W}_F^{t_F} - ^{(k+\alpha)}\mathbf{W}_F^{t_F}||^2, \tag{11}$$

which is an easy to implement expression that provides an optimal value for the relaxation parameter α, at each iterative step.

It is important to note that the relation $0 < \alpha \leqslant 1$ must hold. In the present work, the optimal relaxation parameter is evaluated according to Eq. (11) and if $\alpha \notin (0.01; 1.00)$ the previous iterative-step relaxation parameter is adopted. For the first iterative step, $\alpha = 0.5$ is selected.

4. Numerical aspects and applications

In the next sub-sections some numerical applications are presented, illustrating the potentialities of the proposed methodology. In the first application, a submerged cylinder subjected to an externally applied source is studied. In the second example, a dam-reservoir system is analysed, taking into account linear and nonlinear behaviour.

For all the applications that follow, within the finite element sub-domains, the Newmark method (trapezoidal rule) is considered for time integration and linear finite elements are adopted. For the boundary

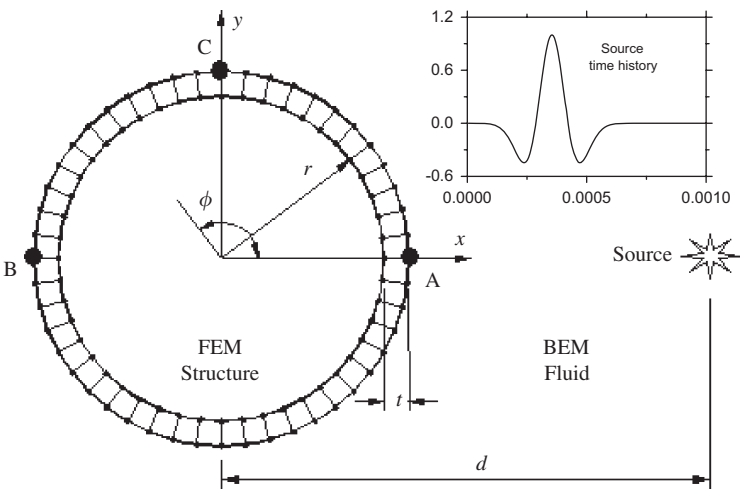

Fig. 1. Submerged cylinder subjected to an external source: sketch of the model.

element sub-domains, spatial discretisation based on linear boundary elements is adopted and linear and piecewise constant time interpolation functions are considered for pressures and fluxes, respectively. The time interpolation/extrapolation procedures related to the boundary element—finite element coupling algorithm are based on the boundary element method time interpolation functions [10]. The convergence of the coupling and/or of the nonlinear iterative process is based on finite element method displacement and residual norms (in the present work, a tight tolerance error of 10^{-5} is adopted). The time-step discretisation within each sub-domain is selected based on the wave propagation velocities involved.

4.1. Submerged cylinder

This example is concerned with the analysis of an elastic infinite cylinder excited by an acoustic wave caused by an external explosion [8,19], as depicted in Fig. 1. The properties of the cylinder are: $E = 2.1 \times 10^{11}\,\mathrm{N/m^2}$

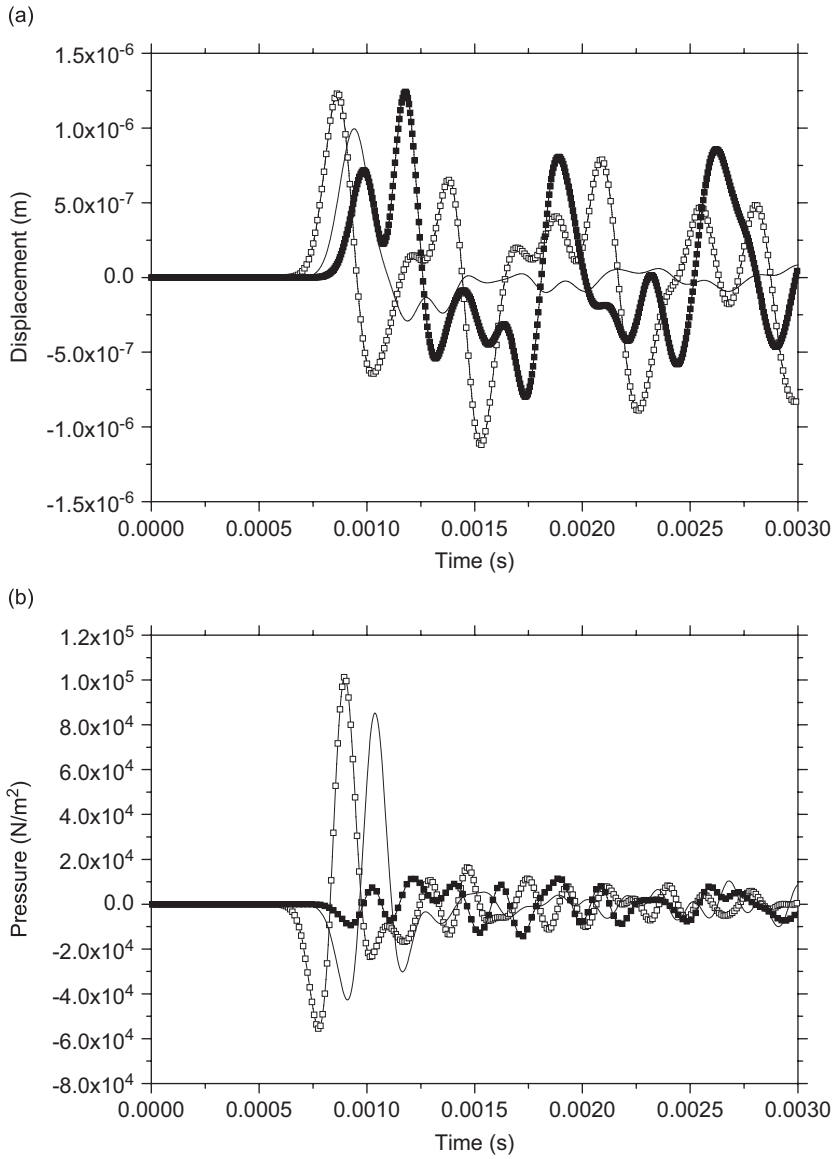

Fig. 2. Time history results at points A, B and C (–□–, point A; –■–, point B; and –––, point C): (a) horizontal displacements and (b) hydrodynamic pressures.

(Young modulus), $v = 0.3$ (Poisson's ratio), $\rho = 7800\,\mathrm{kg/m^3}$ (mass density). The properties of the fluid are: $c = 1524\,\mathrm{m/s}$ (wave velocity), $\rho = 1000\,\mathrm{kg/m^3}$ (mass density). The geometry of the problem is defined by: $r = 0.18\,\mathrm{m}$, $t = 0.0259\,\mathrm{m}$ and $d = 1.0\,\mathrm{m}$. The explosion effects are simulated by the following concentrated source: $S(X,t) = s(t)\delta(X-\xi)$, where δ is the Dirac delta function, $\xi = (d,0)$ and $s(t)$ is depicted in Fig. 1. Forty-eight boundary elements are used to discretise the fluid and forty-eight quadrilateral finite elements are employed to discretise the cylinder. The time-step adopted within the boundary element sub-domain is $\Delta t_B = 0.005\,\mathrm{ms}$; within the finite element sub-domain a time-step $\Delta t_F = 0.001\,\mathrm{ms}$ is adopted.

The horizontal displacement and hydrodynamic pressure time-history results at points A ($\Phi = 0$), B ($\Phi = \pi$) and C ($\Phi = \pi/2$) are depicted in Fig. 2. In Table 2, the average number of iterations per time step and the relative CPU time of the iterative process (both within the time interval $0.5\,\mathrm{ms} < t < 1.0\,\mathrm{ms}$) are presented, considering optimal relaxation parameters (Eq. (11)) and some constant pre-selected α values (the relative CPU time described in Table 2 is computed as the CPU time of the iterative analysis in focus divided by the CPU time of the iterative analysis with optimal relaxation parameters). As it can be observed, optimal relaxation parameters considerably reduce the amount of iterations in the analysis, improving the efficiency and robustness of the methodology.

In Fig. 3, the optimal relaxation parameters, evaluated at each iterative step, are presented. As it can be observed, in the present application, the optimal relaxation parameter varies around very distinct values (according to Fig. 3, it varies mostly around 0.20, 0.55 and 0.95) and a constant pre-selection for α, even when

Table 2
Average number of iterations per time-step and relative CPU time in the submerged cylinder analysis considering optimal and constant pre-selected relaxation parameters.

Relaxation parameter	Average number of iterations per time step	Relative CPU time
0.1	4.14	1.120
0.2	4.02	1.086
0.3	4.00	1.084
0.4	4.01	1.084
0.5	4.04	1.088
0.6	4.04	1.096
0.7	4.02	1.079
0.8	3.98	1.075
0.9	3.84	1.008
1.0	3.98	1.070
Optimal	3.64	1.000

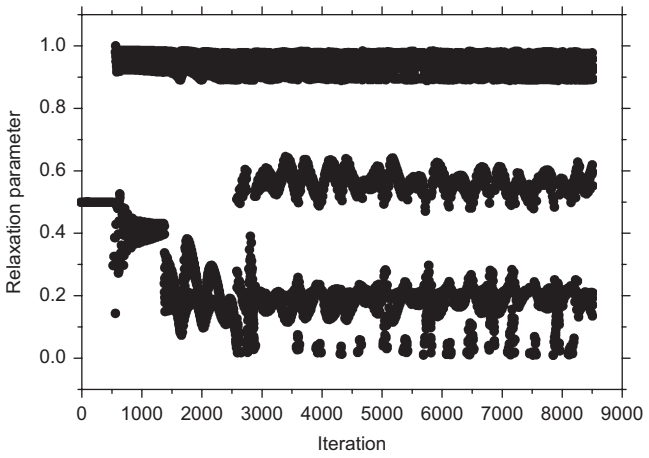

Fig. 3. Optimal relaxation parameters for each iterative step.

most appropriated, is unable to account for this dynamic behaviour. It is important to note that Eq. (11) establishes a correlation between the values of the relaxation parameter and the errors of the iterative procedure, once variable **W** is computed based on iterative residuals (see Eq. (9)).

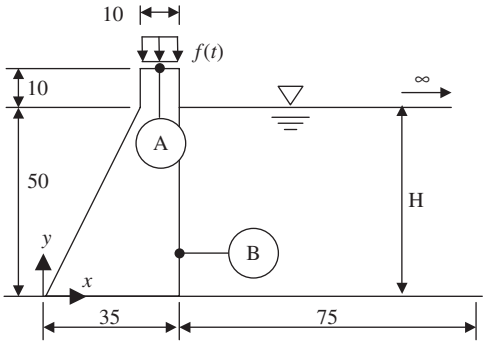

Fig. 4. Dam with a semi-infinite storage-lake: sketch of the model.

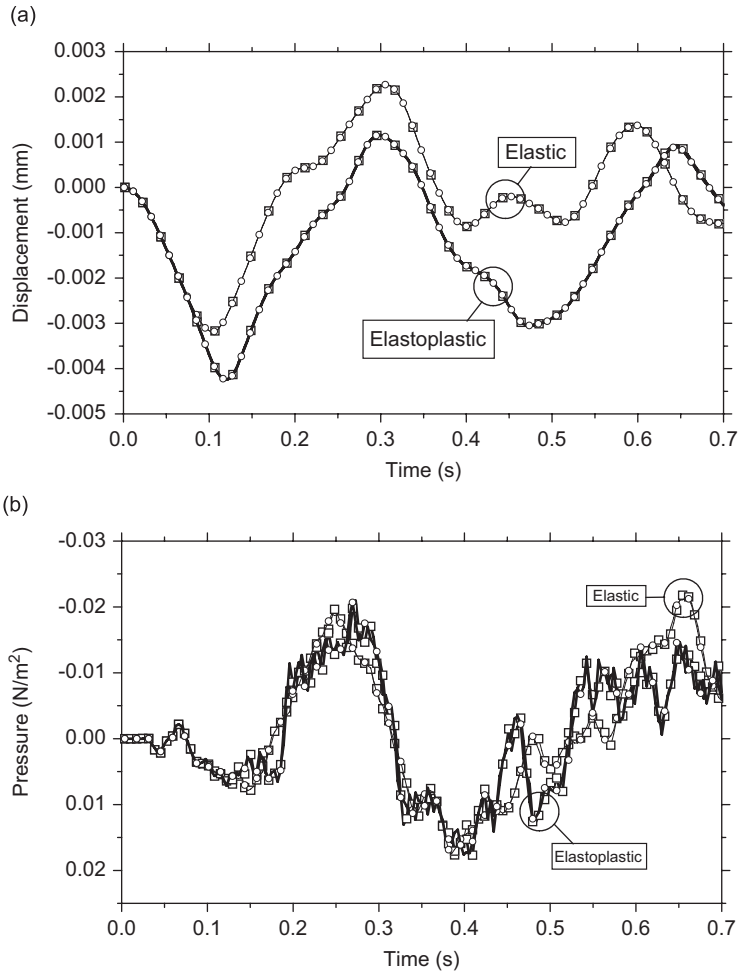

Fig. 5. Time history results considering linear and nonlinear material behaviour (–□–, case 1 and –○–, case 2): (a) vertical displacements at point A and (b) hydrodynamic pressures at point B.

An expression to evaluate the optimal relaxation parameter, properly considering the evolution of the different phenomena involved, is of great importance in order to ensure the effectiveness of the iterative coupling methodology: Eq. (11) provides a simple and easy to implement expression to evaluate efficiently this complex parameter.

4.2. Dam-reservoir system

In this second example, a dam-reservoir system [1,8,10,19,20], as depicted in Fig. 4, is analysed. The structure is subjected to a sinusoidal distributed vertical load on its crest, acting with an angular frequency $w = 18\,\text{rad/s}$. The material properties of the dam are: $E = 3.437 \times 10^9\,\text{N/m}^2$, $v = 0.25$ and $\rho = 2000\,\text{kg/m}^3$ (a perfectly plastic material obeying the von Mises yield criterion is assumed). The adjacent water is characterized by $c = 1436\,\text{m/s}$ and $\rho = 1000\,\text{kg/m}^3$ (a water level defined by $H = 50\,\text{m}$ is considered). Ninety-three quadrilateral finite elements are employed to discretise the dam and the fluid is discretised by constant-length boundary elements ($\ell = 5\,\text{m}$). Regarding temporal discretisation, two cases are here considered, namely: (i) case 1—$\Delta t_B = 0.0035\,\text{s}$ and $\Delta t_F = 0.00175\,\text{s}$; and (ii) case 2—$\Delta t_B = 0.0035\,\text{s}$ and $\Delta t_F = 0.000875\,\text{s}$.

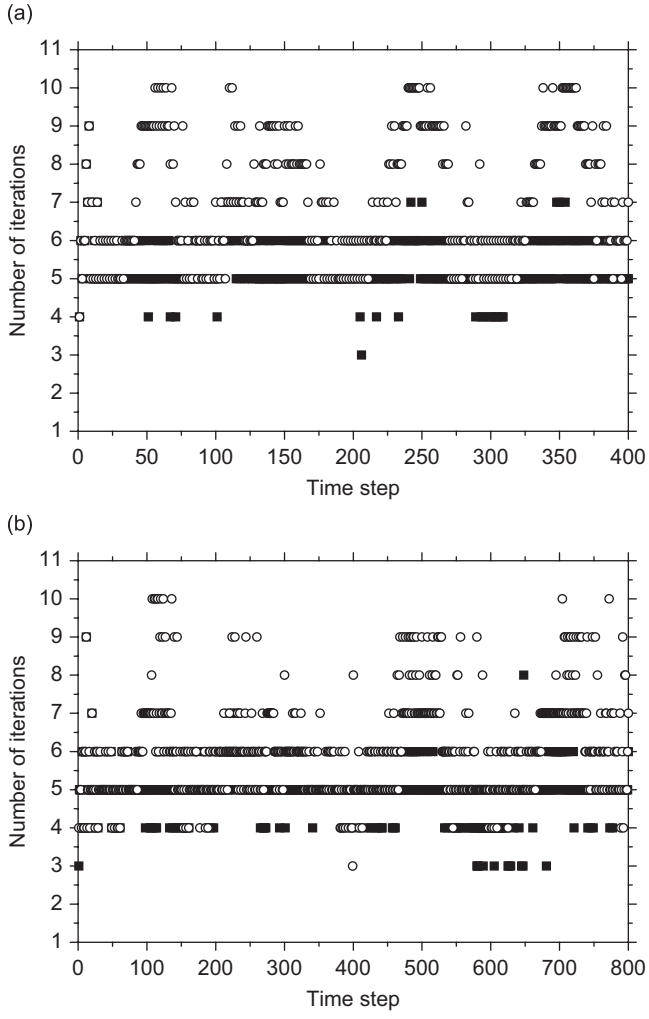

Fig. 6. Number of iterations per time step considering optimal relaxation parameters (■, elastic and ○, elastoplastic): (a) case 1 and (b) case 2.

In Fig. 5, vertical displacements at point A and hydrodynamic pressures at point B are depicted, considering cases 1 and 2, as well as linear and nonlinear analyses. In Fig. 6, the number of iterations per time step is presented, considering optimal relaxation parameters (one should keep in mind that a tight tolerance error is being considered). In Fig. 7, the optimal relaxation parameters, evaluated at each iterative step, are plotted. As can be observed, for the current analyses, the optimal relaxation parameter varies intricately within the interval (0.2; 1.0), illustrating the intense dynamic behaviour of this variable along typical fluid–structure interaction analyses.

In Table 3, the total amount of iterations and the relative CPU time of the iterative process, taking into account nonlinear analyses (cases 1 and 2), are specified. The results are presented considering optimal and some constant pre-selected relaxation parameter values. As can be observed, optimal relaxation parameters reduce the computational cost of the analysis, as well as they ensure convergence in the iterative coupling procedure (in Table 3, the symbol ∞ indicates that convergence is not achieved).

The reader should keep in mind that Eq. (11) requires only very simple vector–vector operations (as for instance, vector subtractions and inner products), taking into account only common interface nodal values. In any iterative step, several vector–vector and matrix–vector operations must be considered in order to numerically analyse the model, taking into account all the nodal values of the problem (which is usually several times greater than the number of the common interface nodal values). As a consequence, the computational effort of computing the optimal relaxation parameter is considerably smaller than that of an

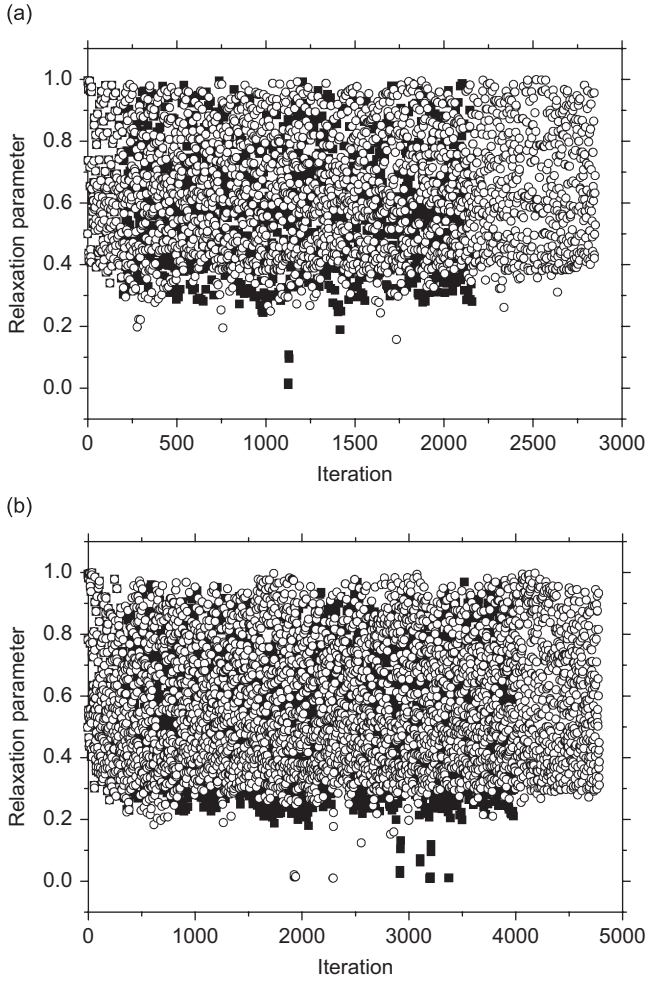

Fig. 7. Optimal relaxation parameters for each iterative step (■, elastic and ○, elastoplastic): (a) case 1 and (b) case 2.

Table 3
Total number of iterations and relative CPU time in the dam-reservoir system nonlinear analyses considering different relaxation parameter values.

Relaxation parameter	Total number of iterations		Relative CPU time	
	Case 1	Case 2	Case 1	Case 2
0.3	3278	4885	1.186	1.058
0.6	3526	∞	1.294	∞
0.9	∞	∞	∞	∞
Optimal	2825	4757	1.000	1.000

extra iterative step, and the reduction of the number of iterations is mandatory for the efficiency of methodology. For problems with a large number of degrees of freedom, the overhead of determining the optimal relaxation parameter is even less significant, since the overburden of evaluating an extra iterative step is much more expressive. Moreover, it must be highlighted that a constant pre-selected value for the relaxation parameter does not ensure convergence (as it is illustrated in the present application) and an optimal relaxation parameter technique must be employed not only to improve the efficiency of the methodology, but also its robustness.

5. Conclusions

In the present work, an optimised boundary element—finite element coupling algorithm to analyse fluid–structure interaction problems is discussed. A simple and efficient expression for an optimal relaxation parameter is proposed, improving the effectiveness and robustness of the time-domain iterative coupling methodology (it is important to observe that, in applications such like fluid–structure interaction problems, a priori good selection for α is hardly trivial and an inappropriate value may very easily invalidate convergence). At the end of the paper, numerical examples are presented, briefly illustrating the potentialities of the described coupling technique (efficiency, accuracy, stability, flexibility etc.) and highlighting the complexity of the optimal relaxation parameter evolution, according to different cases of analysis.

The present methodology improves previous works on the topic (i.e., concerning iterative coupling of hyperbolic time-domain models) and it is a step forward regarding the advance of boundary element—finite element coupling techniques.

Acknowledgements

The financial support by CNPq (Conselho Nacional de Desenvolvimento Científico e Tecnológico) and FAPEMIG (Fundação de Amparo à Pesquisa do Estado de Minas Gerais) is greatly acknowledged.

References

[1] O. von Estorff, H. Antes, On FEM–BEM coupling for fluid–structure interaction analysis in the time domain, *International Journal for Numerical Methods in Engineering* 31 (1991) 1151–1168.
[2] O. von Estorff, Coupling of BEM and FEM in the time domain: some remarks on its applicability and efficiency, *Computer & Structures* 44 (1992) 325–337.
[3] O. Czygan, O. von Estorff, FEM/BEM coupling for fluid–structure interaction including nonlinear effects, *Proceedings of the BEM 22 Conference*, Cambridge, September 2000.
[4] S.T. Lie, G.Y. Yu, Z. Zhao, Coupling of BEM/FEM for time domain structural–acoustic interaction problems, *Computer Modeling in Engineering & Science* 2 (2001) 171–181.
[5] G.Y. Yu, S.T. Lie, S.C. Fan, Stable boundary element method/finite element method procedure for dynamic fluid–structure interactions, *Journal of Engineering Mechanics* 128 (2002) 909–915.
[6] O. Czygan, O. von Estorff, Fluid–structure interaction by coupling BEM and nonlinear FEM, *Engineering Analysis with Boundary Elements* 26 (2002) 773–779.

[7] O. Czygan, Fluid/structure coupling of 2D and axisymmetric systems taking into account a nonlinear structural behaviour (in German), PhD Thesis, TU Hamburg-Harburg, Germany, 2002.
[8] D. Soares Jr., Dynamic analysis of non-linear soil–fluid–structure coupled systems by the finite element method and the boundary element method (in Portuguese), PhD Thesis, Federal University of Rio de Janeiro, Brazil, 2004.
[9] D. Soares Jr., O. von Estorff, Combination of FEM and BEM by an iterative coupling procedure, *Proceedings of the ECCOMAS 2004 Congress*, Jyväskylä, Finland, July 2004.
[10] D. Soares Jr., O. von Estorff, W.J. Mansur, Efficient nonlinear solid–fluid interaction analysis by an iterative BEM/FEM coupling, *International Journal for Numerical Methods in Engineering* 64 (2005) 1416–1431.
[11] W.M. Elleithy, H.J. Al-Gahtani, M. El-Gebeily, Iterative coupling of BE and FE methods in elastostatics, *Engineering Analysis with Boundary Elements* 25 (2001) 685–695.
[12] W.M. Elleithy, M. Tanaka, BEM–BEM coupling and FEM–BEM coupling via interface relaxation, *Journal of Boundary Element Methods* 19 (2002) 37–42.
[13] W.J. Mansur, A time-stepping technique to solve wave propagation problems using the boundary element method, PhD Thesis, University of Southampton, England, 1983.
[14] J. Dominguez, *Boundary Elements in Dynamics*, Computational Mechanics Publications, Southampton, Boston, 1993.
[15] T.J.R. Hughes, *The Finite Element Method*, Dover, New York, 1987.
[16] K.J. Bathe, *Finite Element Procedures*, Prentice-Hall, Englewood Cliffs, NJ, 1996.
[17] M.A. Crisfield, *Non-linear Finite Element Analysis of Solid Structures*, Vols. 1 and 2, Wiley, Chichester, 1991.
[18] T. Belytschko, W.K. Liu, B. Moran, *Nonlinear Finite Elements for Continua and Structures*, Wiley, New York, 2000.
[19] D. Soares Jr., W.J. Mansur, An efficient time-domain BEM/FEM coupling for acoustic–elastodynamic interaction problems, *Computer Modeling in Engineering & Science* 64 (2005) 1416–1431.
[20] D. Soares Jr., W.J. Mansur, Dynamic analysis of fluid–soil–structure interaction problems by the boundary element method, *Journal of Computational Physics* 219 (2006) 498–512.